International Atomic Energy Agency

INDC(CUB)-005
Distrib.: G

INDC INTERNATIONAL NUCLEAR DATA COMMITTEE

CAN BE ACHIEVED A MORE ACCURACY IN NEUTRON CROSS SECTION CALCULATION AT LOW ENERGIES?

R. Cabezas, J. Lubian
Center for Applied Studies to Nuclear Development
Havana, Cuba

March 1992

IAEA NUCLEAR DATA SECTION, WAGRAMERSTRASSE 5, A-1400 VIENNA

INDC(CUB)-005
Distrib.: G

CAN BE ACHIEVED A MORE ACCURACY IN NEUTRON CROSS SECTION CALCULATION AT LOW ENERGIES?

R. Cabezas, J. Lubian
Center for Applied Studies to Nuclear Development
Havana, Cuba

March 1992

CAN BE ACHIEVED A MORE ACCURACY IN NEUTRON CROSS SECTION CALCULATION AT LOW ENERGIES?

R. Cabezas, J.Lubian.
Center for Applied Studies to Nuclear Development
Havana, Cuba

Abstract:

The role of some approximations that traditionally are used in the calculation of neutron inelastic cross section for nuclei in the mass region $48 \leq A \leq 64$ is analyzed. It is shown, that the use of different optical potential parameters for ground and first excited states causes a contribution of more than 10% on the cross section. In the description of the structure of "soft" nuclei, the effect of anharmonicities is considered. This effect has a notable contribution to the cross section near the threshold at low energies. For better description of the experimental data in $^{48}Ti(n,n')$ process, the multi-channel coupled method is used.

I-INTRODUCTION:

At present, an especial attention is devoted to the increase of the accuracy in the calculation and evaluation of nuclear data needed for structural materials. In this sense, different authors work in two directions: the first one related to the creation of new nuclear models for better description of the experimental data and the second one, to the improvement of the existing models.

This second direction has guided the effort of our group in the last few years in the study of the low-energy neutron inelastic scattering process.

In this way, in the frame of the existing nuclear models, additional considerations have been introduced that let us to describe, in a more realistic way, the structure of the target-nucleus (non-axiality, anharmonicity and hexadecapole deformations [1]).

On the other hand, we also analyze how some usual approximations (used to simplify the calculation) can become an obstacle for more accuracy in nuclear data calculation [2].

Between these approaches could be mentioned:

- the use of a spherical optical potential for nuclei that have

permanent or dynamic deformations of its shapes.
- the linear dependence of real potential respect to the energy.
- Non consideration of the influence of direct processes and strong coupling between low-lying states in the calculation of the compound-nucleus cross section.
- the use of the harmonic vibrational model (HVM) for "soft" nuclei in the medium atomic-weight region.
-The use of the same optical potential parameters for each nuclear state of the target nucleus in the neutron inelastic scattering process.
-The use of a few numbers of states in the coupled channel method.

These approximations could give, often, an adequate description in a wide range of energies. Nevertheless, when some of these approaches are extrapolated to low energies, they become improperly because of the growth of collectivity of low-lying states and the strong coupling between excited levels. The use of these simplified models in regions, where the dispersion of experimental data is higher or simply there is not data, is questionable and accuracy of nuclear data obtained by these models is doubtful.

In section II-IV we will refer to some of mentioned above approaches and section V is devoted to the analysis of the strength function calculation using our deformed optical parameterization.

II-Influence of different optical potential parameters for each nuclear excitation level of the target in the low-energy neutron cross section calculation.

Usually, in the calculation of the transmission coefficients related to the exit channels by the Hauser-Feshbach formula, it is assumed that the optical potential does not depend on the excitation energy of the target. It is equivalent to take for all the considering excited states the same optical potential parameters used for the ground state.

From the practical point of view it is justified because of the impossibility of measure of experimental data from the excited nuclei [3].

Furthermore, in the coupled-channel equations, for the calculation of the scattering wave functions the same potential parameters are used independently of the excitation energy of the state.

Ref.4 shows that the consideration of this effect has a notable influence on the calculation of neutron strength functions. So, we can

ask the question: could this effect give a substantial influence on the description of neutron cross sections?

To answer this question we have devoted this section.

For this purpose, we analyze the inelastic scattering of some medium mass isotopes and calculate the neutron cross sections.

FORMALISM OF CALCULATION.

The compound nucleus cross sections were calculated using the Hauser-Feshbach formalism including width-fluctuation corrections and corrections due to the presence of direct processes [5]. For the calculation of direct cross section the coupled-channel method [6] was used.

The optical potential was taken in its conventional form, consisting in a real part with the Woods-Saxon form-factor, a surface imaginary part with derivative of the Woods-Saxon form-factor and a real spin-orbital Thomas term. It has the following form:

$$V(r) = U f_u(r) - 4ia_v W_s \frac{df_v(r)}{dr} + \left(\frac{h^2}{m_\pi c}\right)^2 \frac{1}{r} U_{so} \frac{df_{so}(r)}{dr} (\hat{L}\cdot\hat{\sigma}), \qquad (1)$$

where U, W_s and U_{so} are the depths of real, surface imaginary and spin-orbital potentials, respectively;

$$f_i(r) = [1+\exp((r-R_i)/a_i)]^{-1},$$

is the Woods-Saxon form-factor; a_i and $R_i=r_iA^{1/3}$ are the diffusenesses and reduced radii of the corresponding potentials.

The calculation was carried out using the deformed optical model parameterization obtained by the authors in Ref. 1 for medium mass nuclei at low-energies expressed as:

$$\begin{aligned} U &= 52.095 - 0.735E - 0.195E^2 - 11.528\cdot[1-0.171E]\eta \\ W_s &= 0.343 - 0.337E + 0.304E^2 - 1.234\cdot[1-1.366E]\eta \\ a_v &= a_{so} = 0.645 \text{ f} \\ r_v &= r_s = r_{so} = 1.244 \text{ f} \\ a_s &= 0.434 \text{ f} \\ V_{so} &= 7.418 \text{ MeV}, \end{aligned} \qquad (2)$$

where E is the incident energy and η the isotopic factor (N-Z)/A.

The wave function of the harmonic vibrator considering one-phonon and two-phonon excitations was taken as a basis wave function in the coupled channel equation. In this sense, the expansion of the nuclear

radius in spherical harmonics was considered up to the quadrupole term:

$$R_i = r_i \left[1 + \beta_2 Y_{20} \right] \qquad (3)$$

Parameters β_2 for different isotopes were taken from Ref.7 considering the normalization to the radius r_i used in this work. For the coupled scheme, the first 6 low-lying states of involved nuclei were taken into account. The rest of the states were taken as uncoupled.

RESULTS AND DISCUSSION.

The influence of different potential parameters for each nuclear level in the cross section calculation was studied assigning two set of parameters to the ground and first excited state respectively. For this purpose the parameterization (2) was used. The energy appearing in this formulae was taken as:

$$E_n = E - \omega_n,$$

where E is the incident neutron energy and ω_n is the energy of the first excited state. In this way were calculated the coupling potentials for each channel and the transmission coefficients corresponding to the scattering of the particle in an excited nuclear state. This is equivalent to consider that the ground state of the target was moved to its n excited state.

This consideration was made only for the first excited state 2_1^+. The other ones, for simplicity, were taken with the same potential parameters that 2_1^+ state. Certainly, the cross section corresponding to the 2_1^+ state gives the more relevant contribution to the total cross section.

Calculations were carried out for $^{50,52}Cr$, ^{56}Fe, $^{58,60}Ni$ and ^{48}Ti isotopes. For this purpose, the ECIS code was used [8].

Figs. 1-12 show the angular distributions. Full line shows the calculations made with the same potential parameters for all levels and dashed line, with two different set of parameters for ground and excited states respectively. It can be seen that the consideration of different potential parameters brings on a significant decrease in the most of the angular distributions of the 2_1^+ state obtaining a good agreement with the experiment.

For elastic differential cross sections it can be observed a right shift of the first minimum in the curve reaching a good agreement with the experiment.

In figs. 13-20, the calculations of the integral and total cross sections with different potential parameters (dashed line) and with the same one (full line) are shown. It can be observed that the biggest influence appears at energies close to the 2_1^+ state energy. The difference in a lot of cases reaches more than 10% of its initial value. With the increase of the energy, this difference can be neglected (see tables 1-3).

Energy	Isotopes							
	^{56}Fe		^{48}Ti		^{54}Cr		^{50}Cr	
	1 pot	2 pot	1 pot	2 pot	1 pot	2 pot	1 pot	2 pot
1.9	3.531	2.942	-	-	3.444	3.025	3.523	4.047
2.0	3.448	2.984	4.245	3.884	3.441	3.021	3.519	3.902
2.2	3.340	3.060	4.228	3.733	3.450	3.053	3.650	3.801
2.4	2.966	3.123	4.158	3.677	3.477	3.075	3.594	3.649
2.6	2.939	3.176	4.127	3.717	3.505	3.119	3.605	3.583
2.8	3.245	3.274	4.107	3.809	3.527	3.140	3.592	3.563
3.0	-	-	4.095	3.909	3.531	3.245	3.362	3.263

Table 1: Comparison of the total cross sections (in barns) calculated with the same optical potential parameters for all nuclear levels (1 pot) and with different ones (2 pot) for some studied isotopes.

Energy	Isotopes							
	^{56}Fe		^{48}Ti		^{54}Cr		^{50}Cr	
	1 pot	2 pot	1 pot	2 pot	1 pot	2 pot	1 pot	2 pot
1.9	2.193	2.431	-	-	2.585	2.381	2.623	3.097
2.0	2.180	2.527	3.173	3.035	2.550	2.331	2.606	2.955
2.2	2.179	2.539	3.158	2.951	2.508	2.245	2.850	2.823
2.4	2.254	2.291	3.086	2.463	2.481	2.281	2.576	2.723
2.6	2.280	2.247	2.979	2.836	2.516	2.327	2.563	2.663
2.8	2.307	2.420	2.939	2.847	2.486	2.305	2.543	2.641
3.0	-	-	2.929	2.886	2.448	2.344	2.419	2.481

Table 2: Comparison of the integral elastic cross sections (in barns) calculated with the same optical potential parameters for all nuclear levels (1 pot) and with different ones (2 pot) for some studied isotopes.

Energy	Isotopes							
	^{56}Fe		^{48}Ti		^{54}Cr		^{50}Cr	
	1 pot	2 pot	1 pot	2 pot	1 pot	2 pot	1 pot	2 pot
1.9	745.3	865.5	-	-	851.7	638.8	899.8	971.4
2.0	777.7	895.5	1036.6	851.0	861.6	678.9	908.9	929.0
2.2	769.9	750.3	1069.8	779.9	868.0	667.7	772.1	882.3
2.4	819.2	565.6	1014.1	675.1	818.9	723.7	872.7	852.0
2.6	799.9	621.9	900.3	681.1	841.3	712.3	863.0	826.8
2.8	767.7	677.6	871.9	696.2	763.0	628.6	855.6	725.3
3.0	-	-	856.3	700.8	718.9	639.0	712.8	639.6

Table 3: Comparison of the integral inelastic (2_1^+ state) cross sections (in millibarns) calculated with the same optical potential parameters for all nuclear levels (1 pot) and with different ones (2 pot) for some studied isotopes.

Furthermore, we analyze the influence of different potential parameters on the direct and compound part of the integral cross section for the ground and 2_1^+ states. The result of this analysis is shown in figs. 21-26. It can be noted a decrease of the compound part and a growth less relevant of the direct part.

With the growth of energy both parts have the same values but opposite sign (see figs. 21-26).

III-Influence of anharmonic effects in the neutron cross section calculation.

The low-lying levels of nuclei in the 1f-2p shell suggest features intermediate between harmonic vibrators and rigid rotators and exhibit many properties characteristic of nuclei "soft" to collective motion [21-25].

The static moments provide a sensitive measure for the deformation of the nuclear surface and suggest for the stable even titanium isotopes a transition from appreciable permanent deformation (^{46}Ti) to an almost spherical shape (^{50}Ti) [26]. Moreover, results obtained by Guss P.P. *et al.* in Ref.24, suggest a non-spherical shape for the 2^+ excited state, that is in consistence with coulomb excitation measurements in $^{58,60}Ni$ isotopes. On the other hand, it was found, that it was vital to consider an admixture of amplitude of a state of one-phonon character to the amplitude of each triad state in the ^{60}Ni target, in order to get satisfactory agreement with the experimental cross sections [27].

These evidences in the literature show, that there are not such harmonic vibrational nuclei in nature and thus, the use of this approach may lead disagreement with experiment.

In Ref.28 are detailed analyzed two forms of anharmonicities that may be considered in the neutron cross section calculation:
A) anharmonicities due to the neglected higher-order terms in the harmonic vibrational model Hamiltonian,
B) anharmonicities due to the different deformation parameters corresponding to transitions between vibrational levels.

Here we show some of the results of the inclusion of anharmonic effects in neutron cross section.

Neutron cross section calculation was carried out using the deformed optical parameterization obtained by Cabezas R. *et al* in Ref.2 and slightly modified by the inclusion of more realistic deformation parameters for each nuclear state taken into account in the coupling scheme:

$$
\begin{aligned}
V &= 52.351 - 0.655E + 0.026E^2 - 3.37(1 + 0.2412E)\eta \quad [\mathrm{MeV}] \\
W_s &= 1.233 + 0.53E + 0.045E^2 + 1.01(1 - 0.383E)\eta \quad [\mathrm{MeV}] \\
V_{so} &= 7.418 \quad [\mathrm{MeV}]
\end{aligned}
\qquad (4)
$$

$$r_v = r_w = r_{so} = 1.24 \text{ fm}$$

$$a_v = a_{so} = 0.645 \text{ fm}, \qquad a_w = 0.434 \text{ fm}$$

where E is the incident neutron energy and η is the isotopic factor $\eta=(N-Z)/A$.

A detailed explanation of the levels taken into account in the coupling scheme and the characteristic of these states are shown in Ref.28. The calculations were carried out for ^{48}Ti, ^{52,54}Cr, ^{54}Fe, ^{58}Ni isotopes, but we include here some of these results.

In figs.27-38 are shown the results of calculation of differential elastic and inelastic cross section for 2^+_1 state, integral elastic and inelastic and total cross sections. The full line corresponds to the harmonic vibrational model (HVM) calculations, *mixing 1&2 ph. states* means the mixture between the two first 2^+ excited states (case A), *Anharm. vib.* means the differentiation of the transition amplitudes (case B), and *Anharm. + mixing* means taking in a combined way both effects of anharmonicities.

It can be observed that the most influence of these anharmonic effects takes place near the threshold and becomes neglected when the neutron incident energy increases.

It can be observed that the calculations are in agree with the experimental data and in the most cases the consideration of anharmonicities improves this agreement.

E_n	HVM	AVM case A	AVM case B	AVM case A+B
1.1	2872.45	2844.49	2644.94	2926.91
1.2	2916.56	2871.22	2628.32	2865.05
1.4	3037.36	2970.5	2656.36	2812.31
1.6	3080.66	3010.57	2716.58	2796.1
1.8	3049.61	2984.87	2774.81	2785.42
2.0	2991.73	2936.95	2809.17	2763.96
2.3	2951.2	2916.46	2811.57	2713.74
2.6	2919.34	2930.88	2746.43	2693.5
2.7	2894.31	2904.08	2736.89	2679.41
3.3	2796.59	2801.05	2678.94	2631.53
3.6	2669.49	2672.82	2577.19	2535.67
3.9	2550.3	2552.45	2486.17	2447.23
4.5	2398.3	2398.68	2373.4	2341.18
5.0	2290.55	2291.78	2284.84	2275.03

Table 4: Comparison of integral elastic cross section calculations for ^{48}Ti using (HVM) and anharmonic vibrational model (AVM). The incident neutron energy E_n is given in MeV and the cross sections in mb.

E_n	HVM	AVM case A	AVM case B	AVM case A+B
1.1	631.37	592.06	557.34	538.89
1.2	760.87	715.17	652.61	630.65
1.4	897.61	848.25	800.57	765.48
1.6	976.13	924.54	919.32	865.71
1.8	1021.23	969.17	1003.72	934.06
2.0	1033.98	982.63	1050.70	970.08
2.3	988.22	935.28	1045.78	948.21
2.6	845.60	819.03	912.74	858.04
3.3	662.78	659.75	740.26	720.53
3.6	518.27	516.53	593.95	579.21
3.9	402.29	399.72	476.64	460.22
4.5	311.75	306.88	369.99	354.41
5.0	272.63	266.44	316.46	301.76

Table 5: Comparison of integral inelastic cross section calculations for 2_1^+ state of ^{48}Ti using HVM and AVM. The incident neutron energy E_n is given in MeV and the cross sections in mb.

In tables 4 and 5 are shown the influence of both effects on the integral cross section for ^{48}Ti isotope. Here, both anharmonic effects give a significant contribution to the integral elastic and inelastic 2_1^+ cross section.

In the next section, we will analyze how the consideration of many

excited states in the target nucleus influences in the calculation of neutron cross section.

IV-Description of neutron cross section for ^{48}Ti, using the multi-channel coupling method (MCCM)†.

The problem of description of neutron cross sections at low-energies (En < 5 MeV) for nuclei of structural materials (Ti-Ni) in the frame of spherical optical model as well as any variant of coupled-channel method using a few numbers of channels is very difficult. This is a consequence of the shell structure of these nuclei. In spite of this structure, the neutron strength functions have maximum values for even orbital moments and minimum for the odd ones.

Optical potentials parameters, obtained by describing low-energy neutron strength functions, usually, have a little imaginary part (W < 2 MeV) [35]. However, these values are not able to describe neutron cross sections at higher neutron energies. To eliminate this incongruence has been proposed an absorptive potential with radius over the limits of the nucleus [36] and potential with a sharp energy dependence of the diffuseness, when any channel is opened [37]. Nevertheless, the physical meaning of these approaches is not yet clear.

Furthermore, an intermediate structure in the neutron cross sections of these nuclei is observed. Semimicroscopical calculations [38] show that these structures may be recognized as doorway states, originated by one-phonon excitation of the even-even target-nucleus and neutron on the bound or quasi-bound state. Calculations show that isolated doorway states exist only in nuclei with little bound neutron energy and high excitation energy for low-lying one-phonon states (for ex. ^{208}Pb). For most of nuclei in Ti-Ni region, the level density of complex configuration (like 3p-2h) at bound neutron energies is enough high, so doorway states are mixed with more complex states and intermediate structure of the cross section is smoothed.

In Refs.38-39, in the frame of MCCM, an analysis of neutron cross sections and strength functions for some Cr, Fe and Ni isotopes is carried out. In this section, similar analysis for more light nucleus (^{48}Ti) with a high binding neutron energy (Bn = 8.15 MeV) and low excitation energy of low-lying collective states (≈ 1 MeV for 2^+_1 state) is made.

† This section was elaborated in colaboration with Dr. V.G.Pronyaev and V.P.Lunev from the Institute of Power Physics of Obninsk.

CALCULATION AND RESULTS.

Details of the approximation and choice of parameters corresponding to real part of deformed optical potential are shown in Ref.38.

Energy spectrum and deformation parameter of the target nucleus were taken from Ref.8. In table 6 the excited states considered in the coupling scheme and its characteristics are shown. The depth of the imaginary part of optical potential W_s= 0.22 MeV was taken to average the structures with a little width in the cross section (at low-energies), and for consideration of those channels non including in the coupling scheme at given energy. With this W_s was chosen the depth of the real part of the potential to fit the strength functions So and S_1.

I^π	Energy [MeV]		β
2^+	0.9835		.248
4^+	2.2956	2 phonons $2^+ \otimes 2^+$	
2^+	2.4210		
0^+	2.9973		
4^+	3.2398		.15
3^-	3.3588		.18
6^+	3.5110		.019
2^+	3.6180		.038
3^-	3.8560		.010
3^-	4.5910		.017
3^-	5.5370		.11

Table 6: Characteristics of the states taken into account in the coupling scheme.

In previous papers [38,39] the neutron cross sections were calculated with independent of energy surface imaginary potential. For the present nucleus it was necessary to include a little energy dependence to describe the cross section at higher energies. The physical reason of this dependence is well understood. At higher energies many channels are opened and they are not taken into account in the coupling scheme, so they are included implicitly by increasing the imaginary part of the potential.

Optical potential parameters were taken as follows:

$$V_o = 50.1 - .3E \quad MeV \qquad a_o = .52\ fm \qquad r_o = r_v = r_{so} = 1.23\ fm$$
$$W_s = .22 + .2E \quad MeV \qquad a_v = .40\ fm \qquad (5)$$
$$V_{so} = 7.5 \quad MeV \qquad a_{so} = a_o,$$

where E is the incident neutron energy.

In fig.39, the results of calculation of the total cross section in the frame of MCCM (full line) and using the spherical optical model (SOM) [40] (dotted line), are shown.

It can be noted that the calculation with the MCCM fits the mean values of experimental data and the minimum observed in the region near 1 MeV better than those with the SOM.

Furthermore, the neutron strength function S_o and S_1 were calculated using the MCCM. In table 7 a comparison to the experimental data is shown. In can be seen that the agreement is good.

	MCCM	Exp. [41]
S_o	$2.6 \cdot 10^{-4}$	$(4 \pm 1.3) \cdot 10^{-4}$
S_1	$5.8 \cdot 10^{-5}$	$(6 \pm 2) \cdot 10^{-5}$

Table 7: Results of strength function calculation using the MCCM.

V-Strength function calculation.

In this section, we will show a comparison of strength function calculation using the parameterization of deformed optical potential (ec.(4) of section III), with those obtained in the frame of MCCM [42] and with the experimental data (see table 8).

It can be seen that the S_1 strength functions are better described by the CCM, while the S_o strength functions are better fitted by the MCCM. Nevertheless, in general, the strength functions calculated using our parameterization are close to the experimental data. The divergence of our calculations in some cases (for example for ^{54}Fe) may be due to the fact that our parameterization was obtained on the base of the description of the experimental data (angular distributions, excitation functions, etc.) in the energy region 1 - 3 MeV, and not by fitting the strength function.

Target Nucleus	CCM param. ec.4		MCCM [42]		Exp. [41]	
	S_0	S_1	S_0	S_1	S_0	S_1
^{48}Ti	2.83	.82	-	-	4±1.3	.6±.2
^{50}Cr	2.38	.76	4.9	1.34	3.6±.8	.33±.12
^{52}Cr	2.41	.37	4.82	1.15	2.5±.9	.52±.12
^{54}Cr	2.17	.40	3.05	1.17	2.8±1.	-
^{54}Fe	1.68	.22	5.18	.83	8.7±2.4	.58±.11
^{56}Fe	2.05	.29	3.05	.93	2.6±.6	.45±.05
^{58}Ni	2.21	.22	3.01	.81	2.8±.6	.5±.1
^{60}Ni	1.88	.29	2.63	.81	2.7±.6	.3±.1
^{62}Ni	1.66	.29	2.45	.80	2.8±.7	.3±.1
^{64}Ni	1.54	.30	2.43	.79	2.9±.8	.6±.2

Table 8: Comparison of strength function calculation (in units of 10^{-4}) using coupled channel model (CCM) taking the parameterization (4) of sec.III with those using the MCCM and with experimental data.

VI-Conclusions.

From the obtained results we can arrive to the following conclusions:

- The influence of different potential parameters for ground and excited states in the cross sections is more significant at low neutron energies and become neglected with the growth of energy. The contribution of this consideration to the cross sections of the 2_1^+ state is more than 10%. The consideration of this effect provokes an increase of the direct part of the cross section and a decrease of the compound one.
- The included anharmonic effects in the structure of the target nucleus have a notable influence (near to 10%) on total, integral elastic and inelastic cross sections, and angular distributions at low energies (1-5 MeV). It evidences that the HVM in the cases when we need a more accuracy in calculations could be an oversimplified model. The higher influence of studied anharmonic effects is observed near the threshold and decrease with the growth of energy.
- The use of MCCM for the calculation of total cross section of ^{48}Ti allows us to obtain a better description of the mean values of experimental data.
- The description of neutron strength functions using our parameterization for deformed optical potential on the base of HVM

is an additional proof of its consistence for the calculation of inelastic neutron cross section.

REFERENCES.

1. Cabezas R., Progress on nuclear data calculation: Low-energy neutron inelastic scattering. III School on Current Problems in Nuclear Science, 21-26 Oct. 1990, Havana.
2. Cabezas R., Lubian J., Tomas J., INDC(CUB)-002, april 1990.
3. Hodgson P.E., Nuclear Reaction and Nuclear Structure, Clarendon Press, Oxford, 1971.
4. Ignatyuk A.B., Lunev V.P., Neitronnaya Fizika, 1980, part 1, p.77.
5. Moldauer P.A., Phys. Rev. C12 (1975) 744.
6. Tamura T., Rev. Mod. Phys. 37 (1965) 679.
7. Raman S., Malarkey C.H., Milner W.T., Nestor C.W., Stelson P., Atomic Data & Nuclear Data Tables 36 (1987) 1.
8. Raynal J., ECIS87 Code. Unpublished.
9. Korzh I.A. *et al.*, Proc. of the 2nd. All-Union Soviet Conference on Nuclear Physics, Moscow, 1976, part 4, p.229.
10. Korzh I.A. *et al.*, Ukrainsky Fizichesky Zhurnal 22 (1977) 87.
11. Korzh I.A. *et al.*, Proc. of 2nd. National Soviet Conference on Neutron Physics, Obninsk, 1974, part 3, p.56.
12. Broder *et al.*, Voprosy Atommoi Nauky y Tejniky. Seriya: Yadernie konstanty. 10 (1972) 13. (EXFOR40199.009.).
13. Smith ,Nuc. Phys. A307 (1978) 224,. Smith, ANL-NDM-33 1977. Guenther, ANL-NDM-31 1977 (EXFOR10669.002).
14. Almen-Rams., Report AE-503, April 1975.
15. Degtjarev *et al.*, Atomnaya Energiya 23 (1967) 568 N°6
16. Rogers *et al.*, COO Report 1573-33, 1967.
17. Korzh I.A. *et al.*, Ukrainsky Fizichesky Zhurnal 22 (1977) 112.
18. Bultz, Jordensen *et al.*, Z. Phys. A306 (1982) 265. Bultz, Jordensen *et al.*, ANL-NDM-61 1981 (EXFOR12752.006).
19. Harvey., Priv. Comm. Aug./86 (EXFOR12972.001).
20. Rogers *et al.*, Nuc. Sc. and Eng. 45 (1971) 297 (EXFOR10146.004).
21. Frois B., Turck-Chieze S., Bellicard J.B., Huet M., Leconte P., Phan X.H., Sick I., Heisenberg J., Girod M., Kumar K., Grammaticos B., Phys. Lett. 122B (1983) 347.
22. Rebel H., Lohken R., Schweimer G.W., Z. Phys. B256 (1972) 258.
23. Rebel H., Habs D., Phys. Rev. C8 (1973) 1391.
24. Guss P.P., Byrd R.C., Floyd C.E., Howell C.R., Murphy K., Tungate G., Pedroni R.S., Walter R.L., Delaroche J.P., Clegg T.B., Nuc.

Phys. A438 (1985) 187.
25. Mellena S., Finlay R.W., Dietrich F.S., Phys. Rev. C33 (1986) 481.
26. Rebel H., Hauser G.,Schweimer G.W., Nowicki G., Wiesner W., Hartmann D., Nuc. Phys. A218 (1974) 13.
27. Tamura T., Progr. Theor. Phys. Suppl. N°37-38(1966)383.
28. Lubian J.,Cabezas. R., Sended to Journal of Phys. G.
29. Foster O.G. Jr., Glasgow D.W., Phys. Rev. C3 (1971) 576.
30. Mittler P., Privated communication, June 1975. (EXFOR10519.002).
31. Ramstron E.A., Report AE-503, Helsinski, 1975.
32. Guenther P.T.,Smith D.L., Smith A.B., Whalen J.F., Ann. of Nucl. Energy, 13 (1986) 601.
33. Sokolov L.S., Fedorov M.B., Korbetskij E.V., Surovitskaya N.T., Yakovenko T.I., Ukrainsky Fizicheskij Zhurnal, 18(2) (1973) 263.
34. Broder D.L., Kolesov V.E., Lashuk A.I., Sadokhin I.P., Dovbenko A.G., Atomnaya Energiya, 16(2) (1964) 103.
35. Moldauer P.A., Nucl. Phys., 47 (1963) 65.
36. Summary of JENDL-2 General Purpose File, ed. Nakagawa T., JAERI-M -84-103, 1984.
37. Pronyaev V.G. *et al.*, Materials MT= 2610, 2630, 2640, From evaluated data library BROND, 1986.
38. Ignatyuk A.B. *et al.*, Yadernaya Fizika, 50 (1989) 1299.
39. IgnatyuK A.B. *et al.*, Neitronnaya Fizika, !988, part 2, p.70.
40. Korzh I.A., Mishchenko V.A., Yadernaya Fizika, 43 (1986) 1083.
41. Mughabghab S.F., Neutron Cross Sections, V.1, N.Y.-L, Academic Press, 1981.
42. Bychkov V.M. *et al.*, INDC(CCP)-217/LI, IAEA, Vienna, December 1983

FIGURE CAPTIONS

Figs. 1-4: Angular distributions for ^{54}Cr. Experimental data taken from [11].

Figs. 5-8: Angular distributions for ^{48}Ti. Experimental data taken from [10,11].

Figs. 9-10: Angular distributions for ^{50}Cr. Experimental data taken from [11].

Figs. 11-12: Angular distributions for ^{56}Fe. Experimental data taken from [10].

Figs. 13-14: Integral cross sections for ^{54}Cr. Experimental data taken from [11].

Fig. 15: Inelastic cross section for ^{48}Ti. Experimental data taken from: ▲ - [11]; ♦ - [12].

Fig. 16: Total cross section for ^{48}Ti. Experimental data taken from [13] (natural titanium).

Fig. 17: Integral cross section for ^{56}Fe. Experimental data taken from: ● - [10]; ▲ - [14]; ◆ [15]; ■ -[16].

Fig. 18: Inelastic cross section for ^{58}Ni. Experimental data taken from: ▲ -[17]; ● - [18]; ■ - [16].

Fig. 19: Total cross section for ^{58}Ni. Experimental data taken from [19].

Fig. 20: Inelastic cross section for ^{60}Ni. Experimental data taken from: ◆ - [16]; ● - [20].

Fig.1 CR-54, En=2.0 MeV, 0+ g.s.

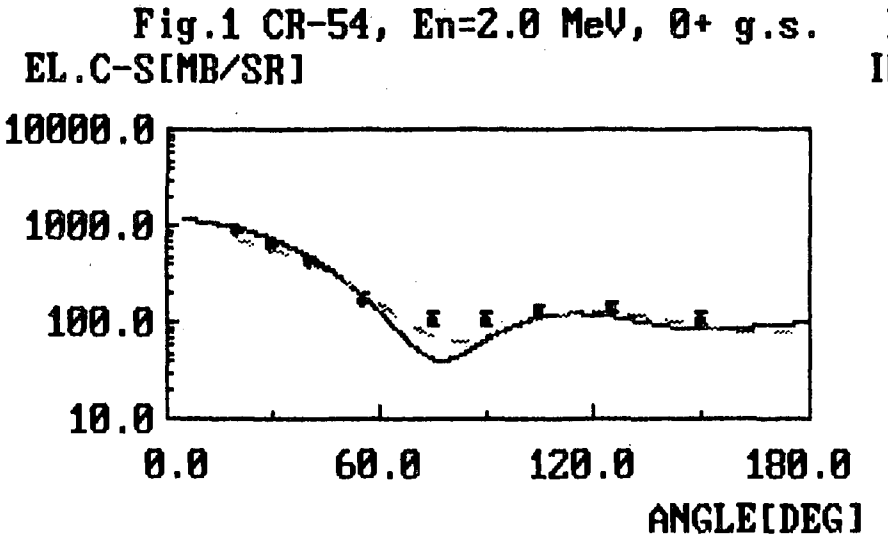

Fig.2 CR-54, En=2.0MeV, 2+(0.835MeV)

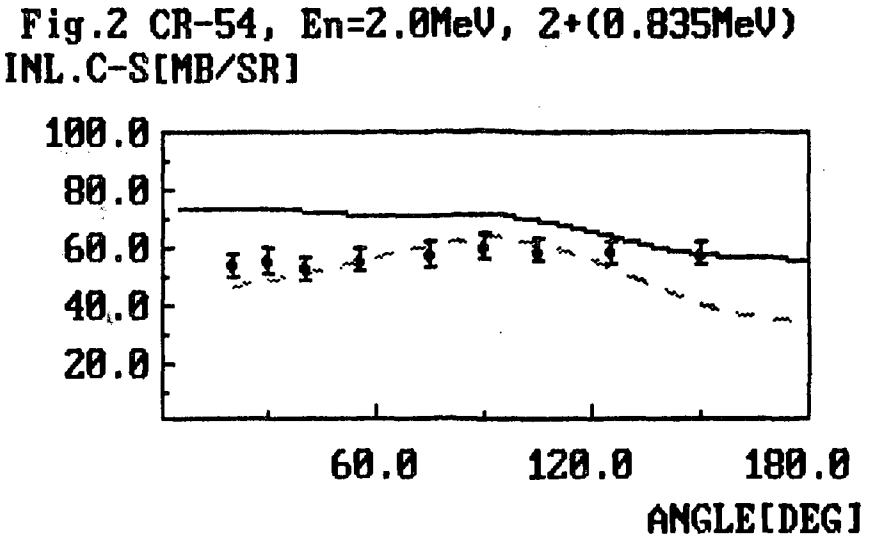

Fig.3 CR-54, En=3.0 MeV, 0+ g.s.

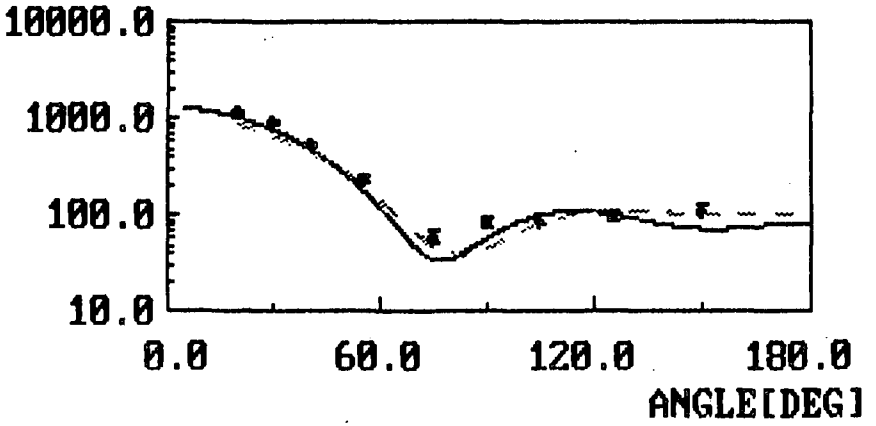

Fig.4 CR-54, En=3.0MeV, 2+(0.835MeV)

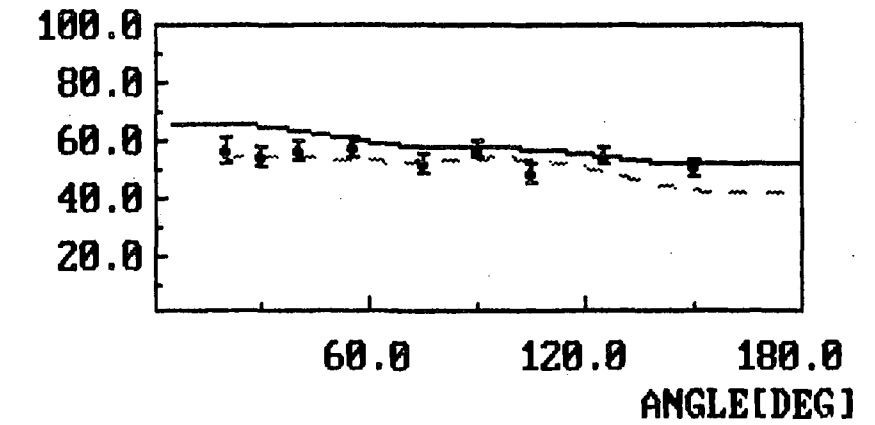

Fig.5 Ti-48, En=2.9 MeV, 0+ g.s.

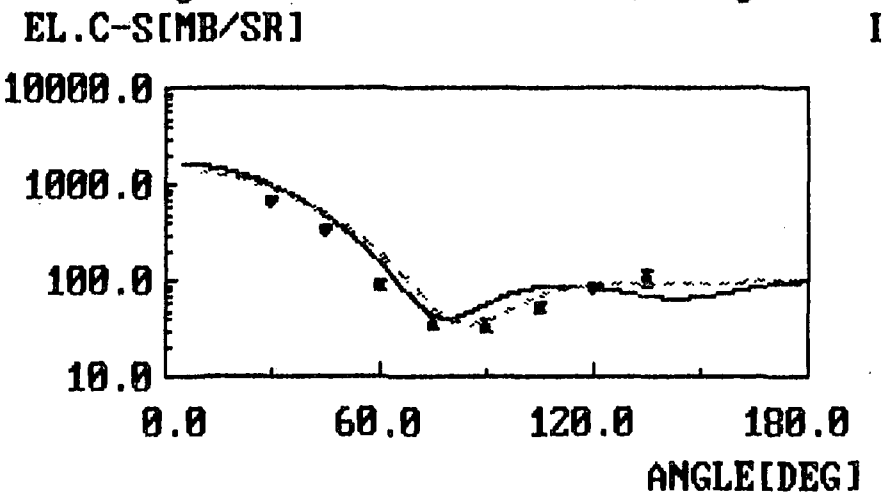

Fig.6 Ti-48, En=2.9MeV, 2+(0.983MeV)

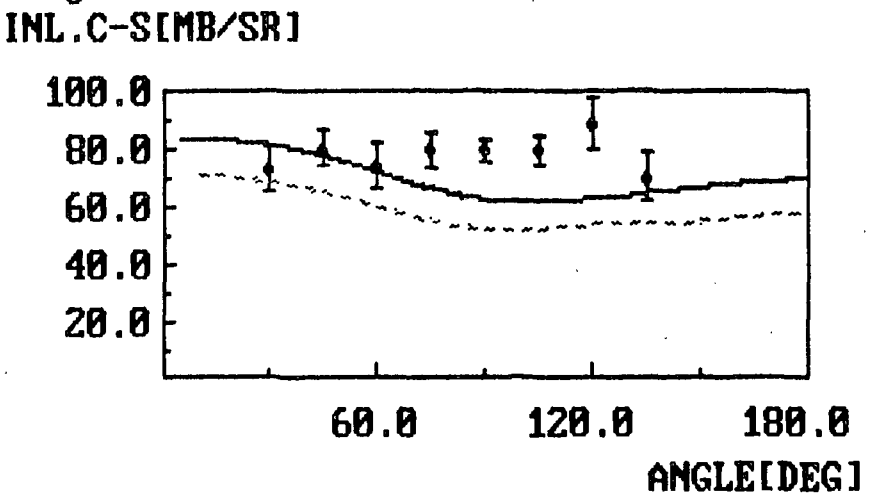

Fig.7 Ti-48, En=3.0 MeV, 0+ g.s.

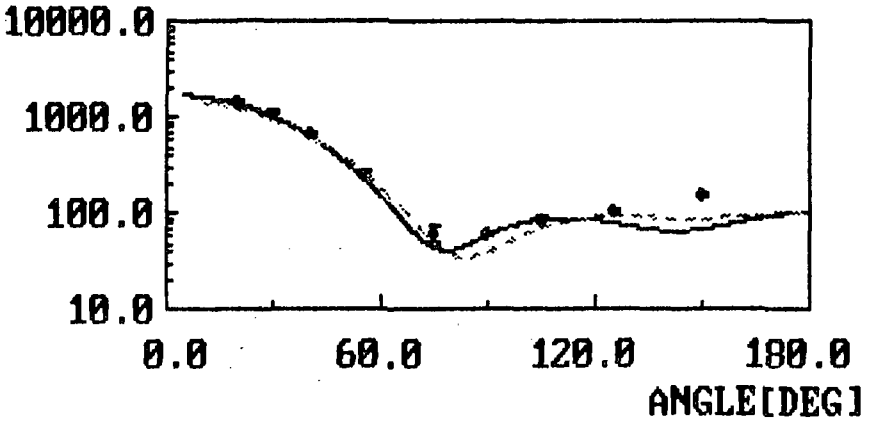

Fig.8 Ti-48, En=3.0MeV, 2+(0.983MeV)

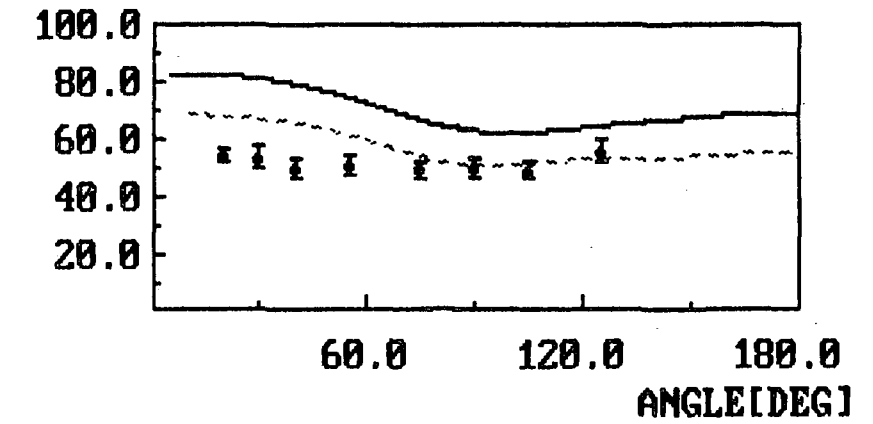

Fig.9 CR-50, En=2.0 MeV, 0+ g.s.

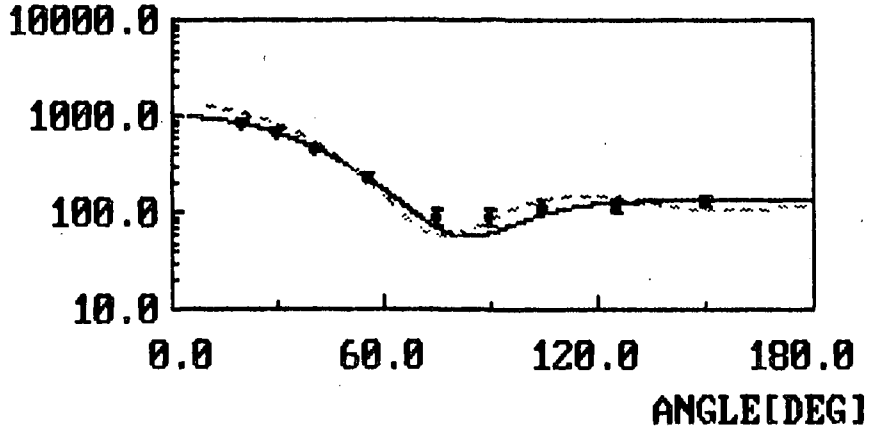

Fig.10 CR-50, En=2.0MeV, 2+(0.783MeV)

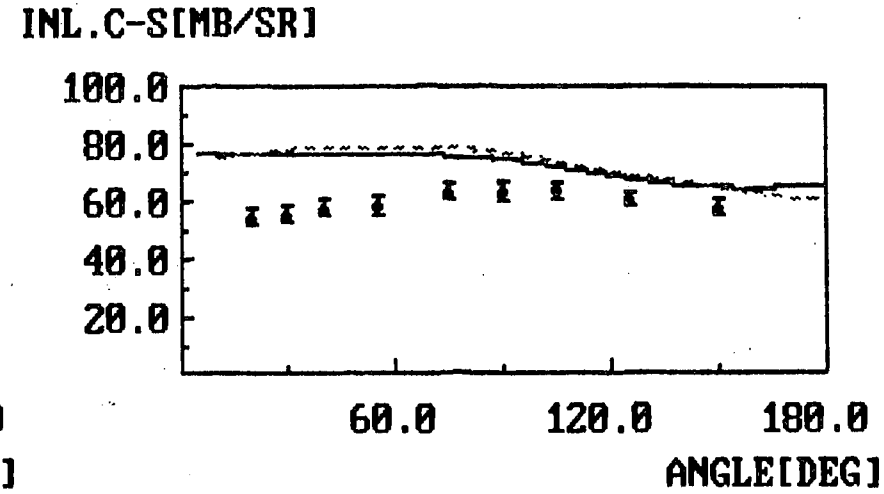

Fig.11 FE-56, En=2.0 MeV, 0+ g.s.

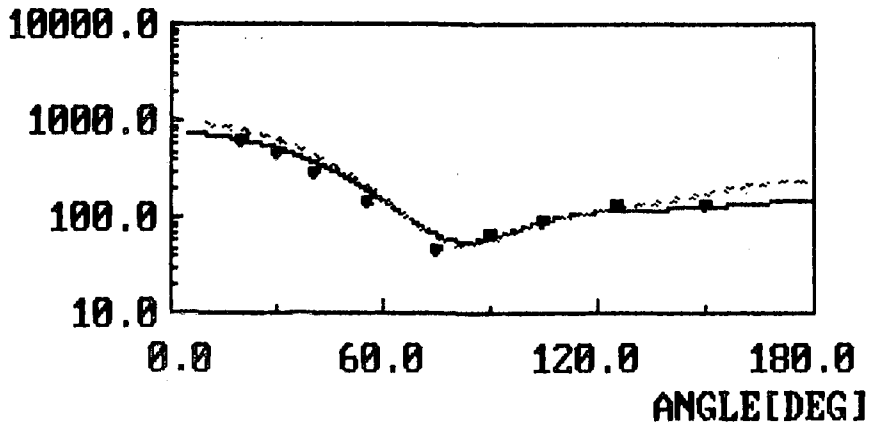

Fig.12 FE-56, En=2.0MeV, 2+(0.847MeV)

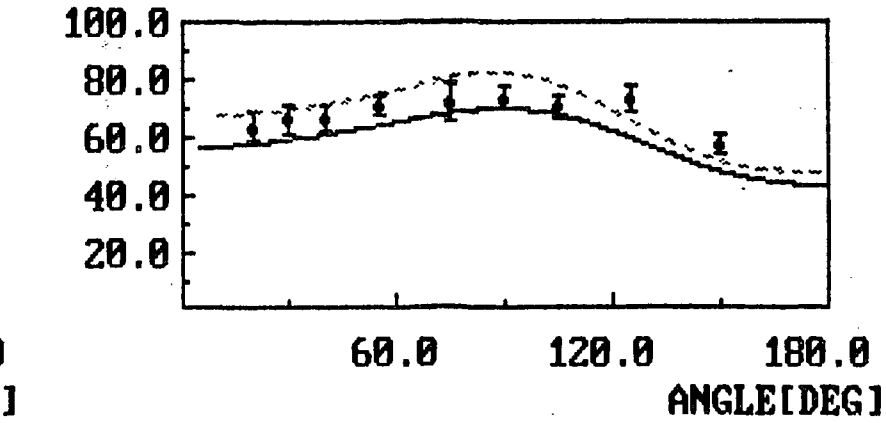

Fig.13 CR-54, INT. CROSS SEC. 0+ g.s.

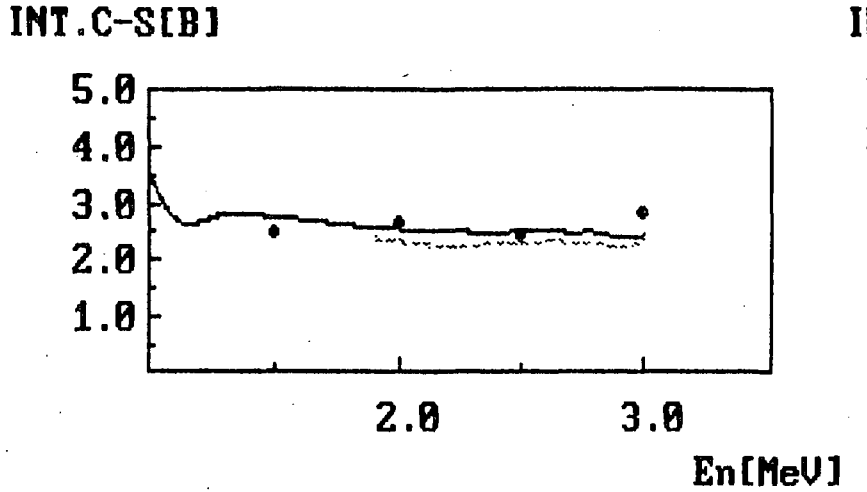

Fig.14 CR-54,INT. CR. SEC. 2+(0.83MeV)

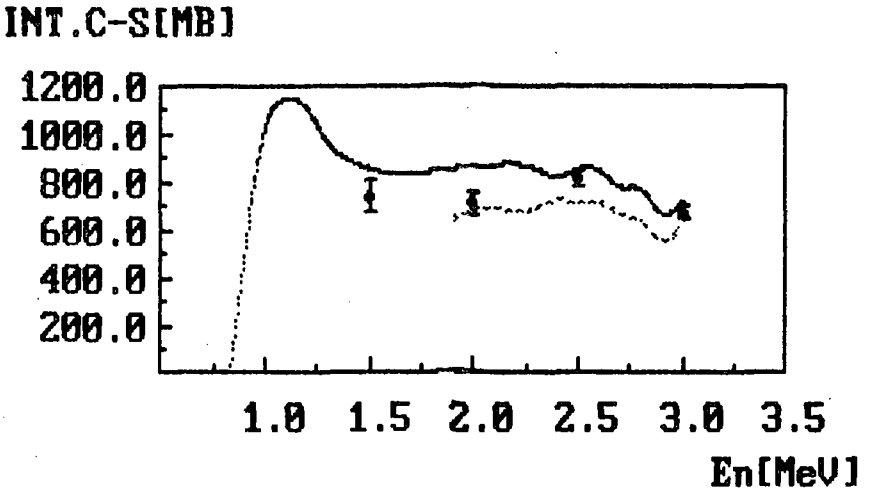

Fig.15 TI-48,INT. CR. SEC. 2+(0.98MeV)

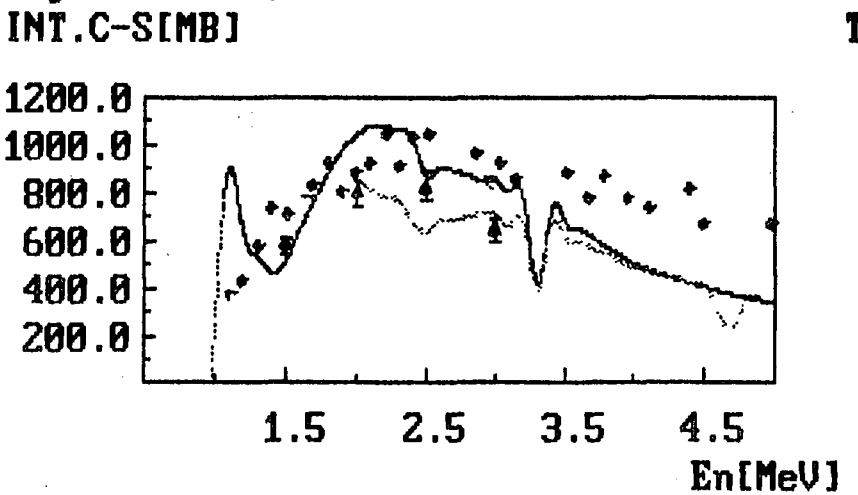

Fig.16 TI-48 TOTAL CROSS SECTION

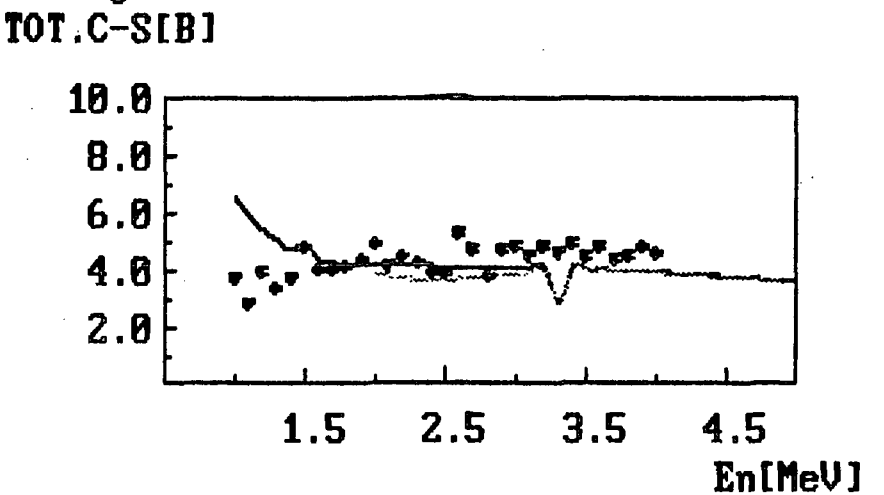

Fig.17 FE-56,INT. CR. SEC. 2+(0.8MeV)
INT.C-S[MB]

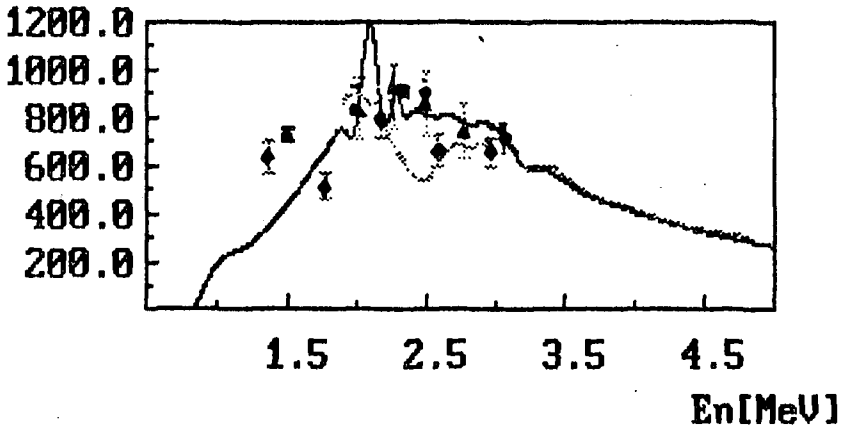

Fig.18 Ni-58,INT. CR. SEC. 2+(1.45MeV)
INT.C-S[MB]

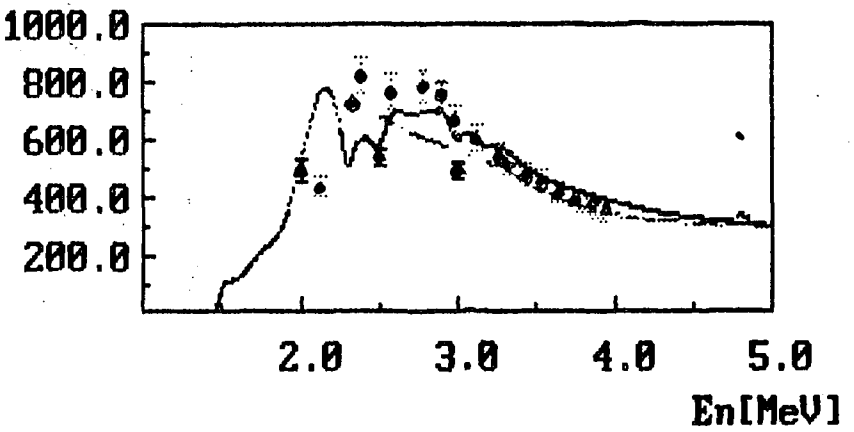

Fig.19 Ni-58, TOTAL CROSS SECTION
TOT.C-S[B]

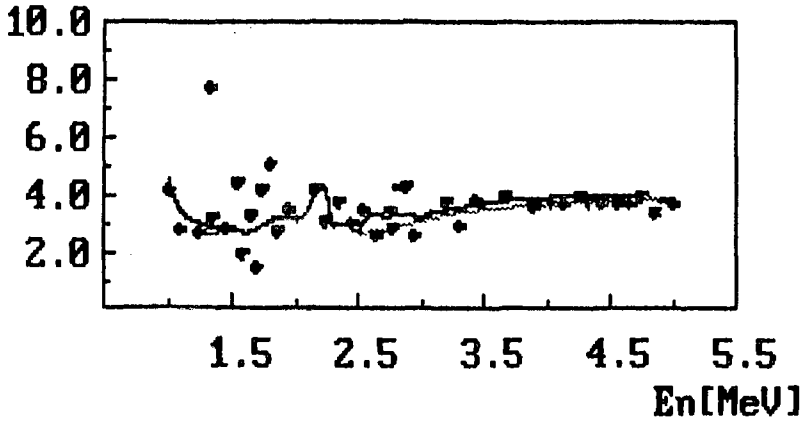

Fig.20 Ni-60,INT. CR. SEC. 2+(1.3MeV)
INT.C-S[MB]

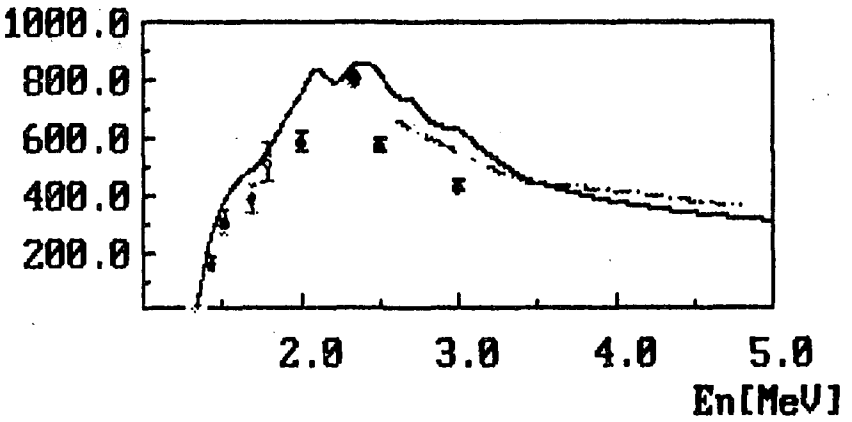

Fig.21
COMP. & DIRECT COMPONENTS OF THE C-S (1 pot- 2 pot)

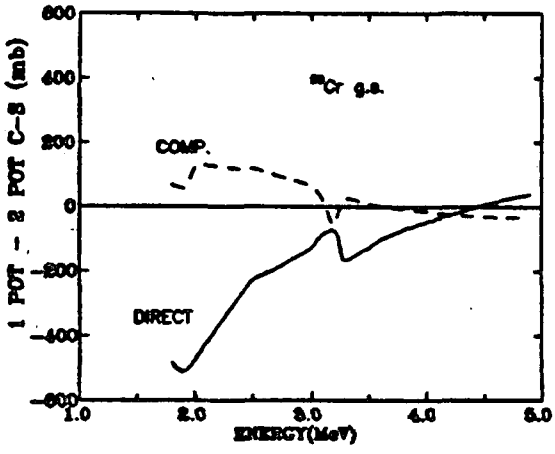

Fig.22
COMP. & DIRECT COMPONENTS OF THE C-S (1 pot- 2 pot)

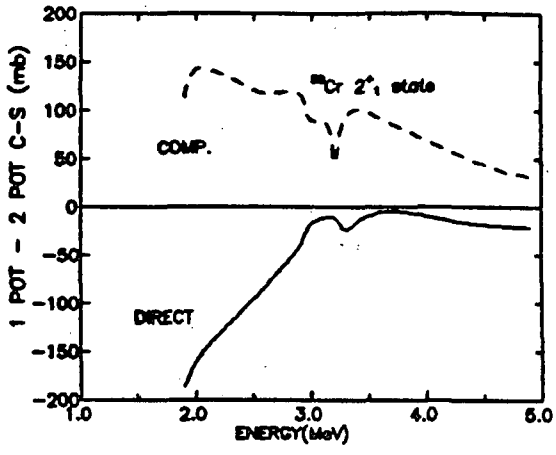

Fig.23
COMP. & DIRECT COMPONENTS OF THE C-S (1 pot- 2 pot)

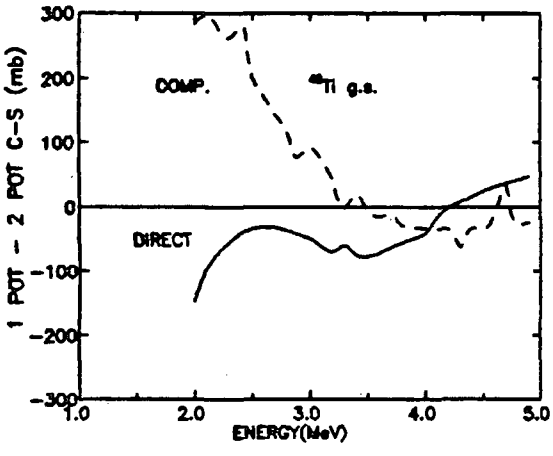

Fig.24
COMP. & DIRECT COMPONENTS OF THE C-S (1 pot- 2 pot)

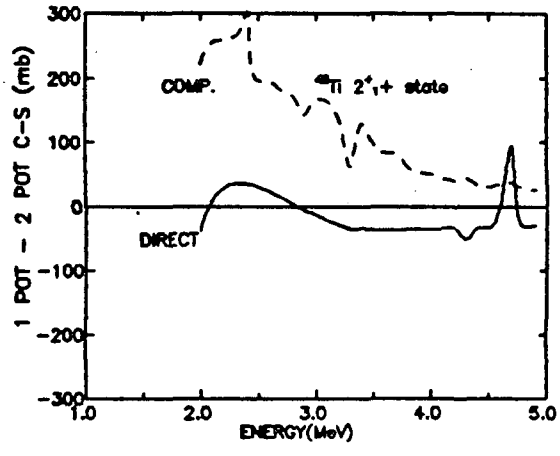

Fig.25
COMP. & DIRECT COMPONENTS OF THE C-S (1 pot- 2 pot)

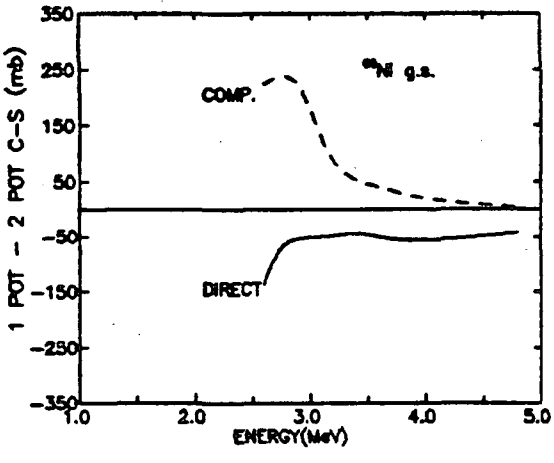

Fig.26
COMP. & DIRECT COMPONENTS OF THE C-S (1 pot- 2 pot)

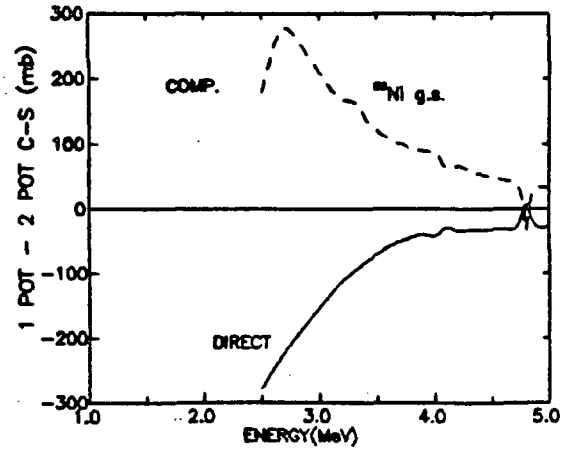

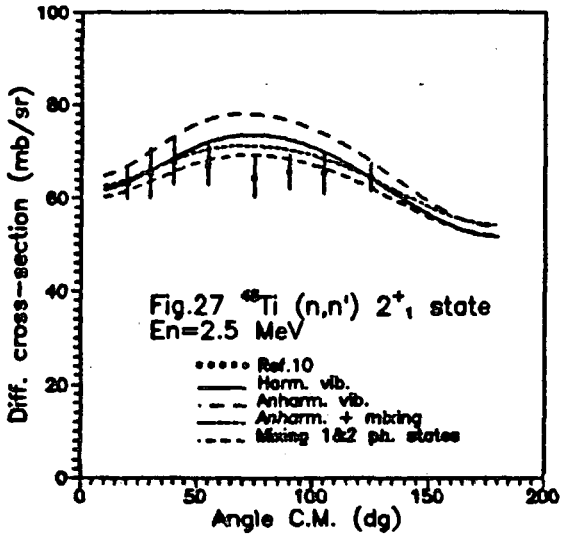
Fig.27 ^{48}Ti (n,n') 2^+_1 state
En=2.5 MeV
Ref.10
Harm. vib.
Anharm. vib.
Anharm. + mixing
Mixing 1&2 ph. states
Diff. cross-section (mb/sr)
Angle C.M. (dg)

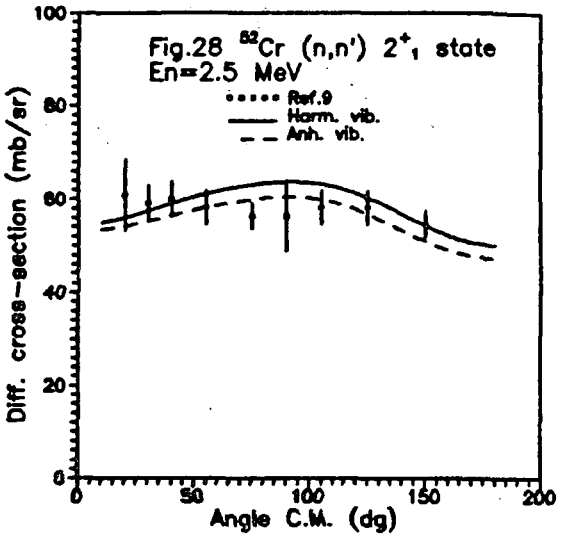
Fig.28 ^{52}Cr (n,n') 2^+_1 state
En=2.5 MeV
Ref.9
Harm. vib.
Anh. vib.
Diff. cross-section (mb/sr)
Angle C.M. (dg)

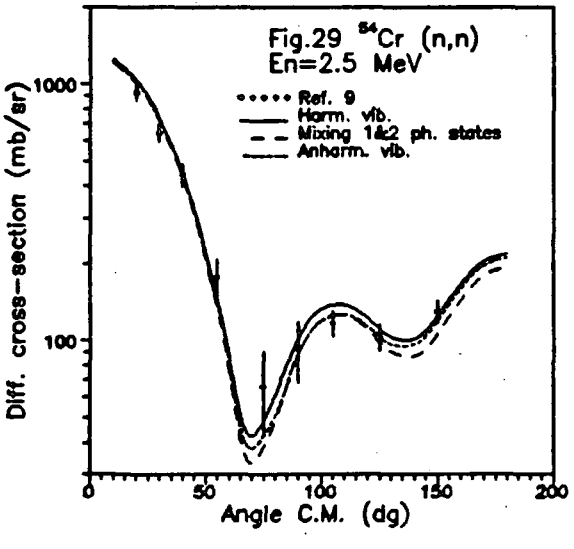
Fig.29 ^{54}Cr (n,n)
En=2.5 MeV
Ref. 9
Harm. vib.
Mixing 1&2 ph. states
Anharm. vib.
Diff. cross-section (mb/sr)
Angle C.M. (dg)

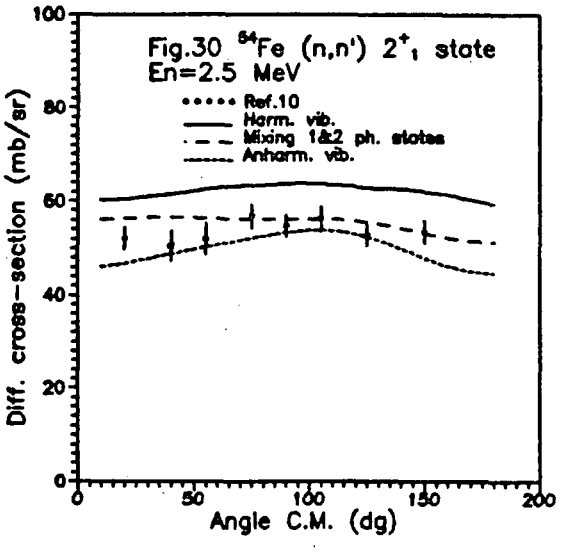
Fig.30 ^{54}Fe (n,n') 2^+_1 state
En=2.5 MeV
Ref.10
Harm. vib.
Mixing 1&2 ph. states
Anharm. vib.
Diff. cross-section (mb/sr)
Angle C.M. (dg)

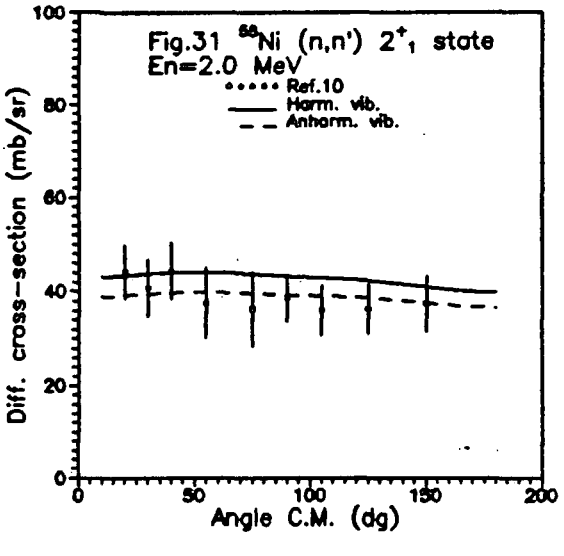
Fig.31 ^{58}Ni (n,n') 2^+_1 state
En=2.0 MeV
Ref.10
Harm. vib.
Anharm. vib.
Diff. cross-section (mb/sr)
Angle C.M. (dg)

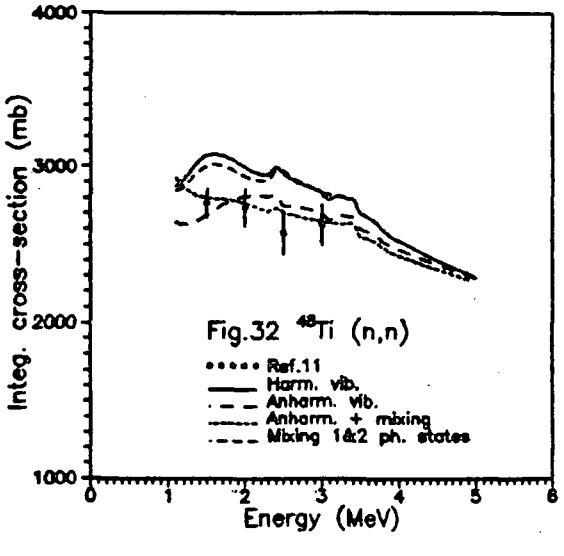
Fig.32 ^{48}Ti (n,n)
Ref.11
Harm. vib.
Anharm. vib.
Anharm. + mixing
Mixing 1&2 ph. states
Integ. cross-section (mb)
Energy (MeV)

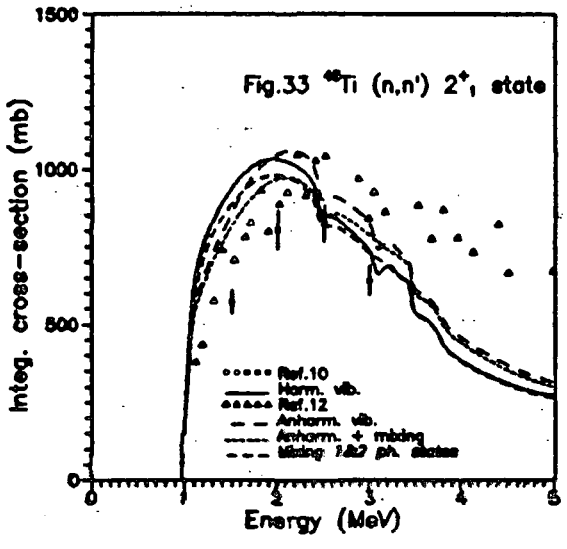
Fig.33 ^{46}Ti (n,n') 2$^+_1$ state
Ref.10
Harm. vib.
Ref.12
Anharm. vib.
Anharm. + mixing
Mixing 1&2 ph. states
Integ. cross-section (mb)
Energy (MeV)

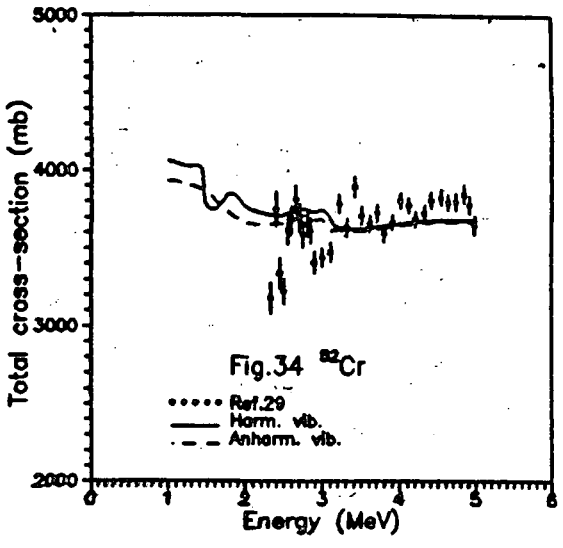
Fig.34 ^{52}Cr
Ref.29
Harm. vib.
Anharm. vib.
Total cross-section (mb)
Energy (MeV)

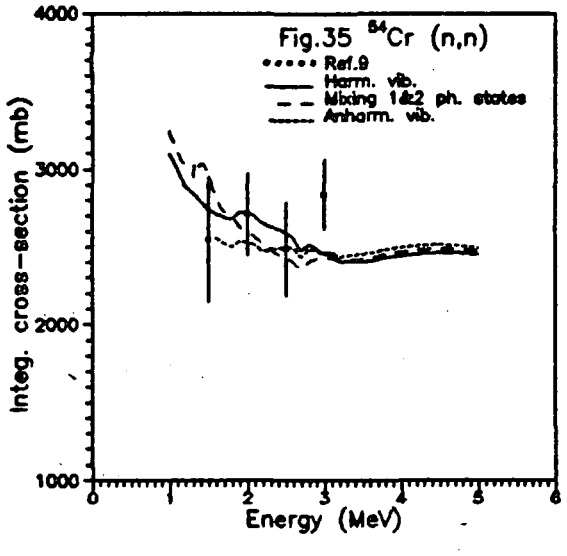
Fig.35 ^{54}Cr (n,n)
Ref.9
Harm. vib.
Mixing 1&2 ph. states
Anharm. vib.
Integ. cross-section (mb)
Energy (MeV)

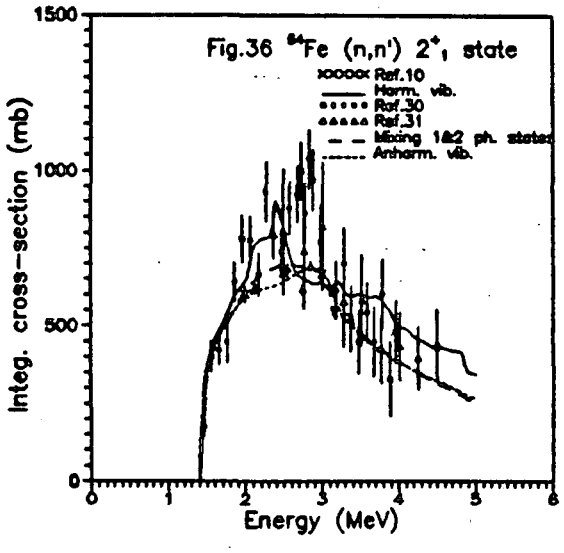
Fig.36 ^{54}Fe (n,n') 2$^+_1$ state
Ref.10
Harm. vib.
Ref.30
Ref.31
Mixing 1&2 ph. states
Anharm. vib.
Integ. cross-section (mb)
Energy (MeV)

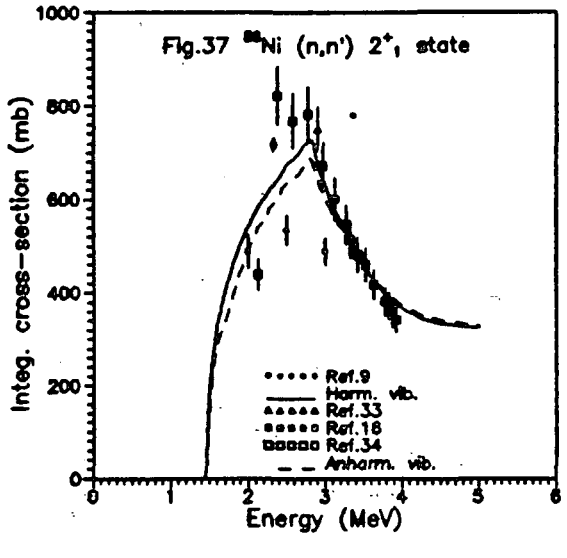
Fig.37 ^{58}Ni (n,n') 2$^+_1$ state
Ref.9
Harm. vib.
Ref.33
Ref.18
Ref.34
Anharm. vib.
Integ. cross-section (mb)
Energy (MeV)

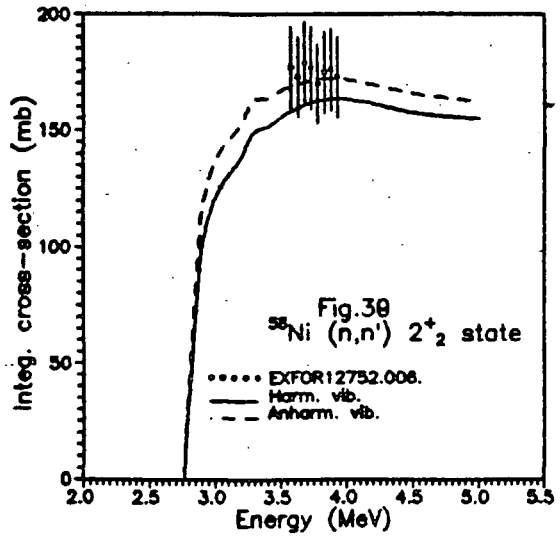
Fig.38
^{58}Ni (n,n') 2$^+_2$ state
EXFOR12752.006.
Harm. vib.
Anharm. vib.
Integ. cross-section (mb)
Energy (MeV)

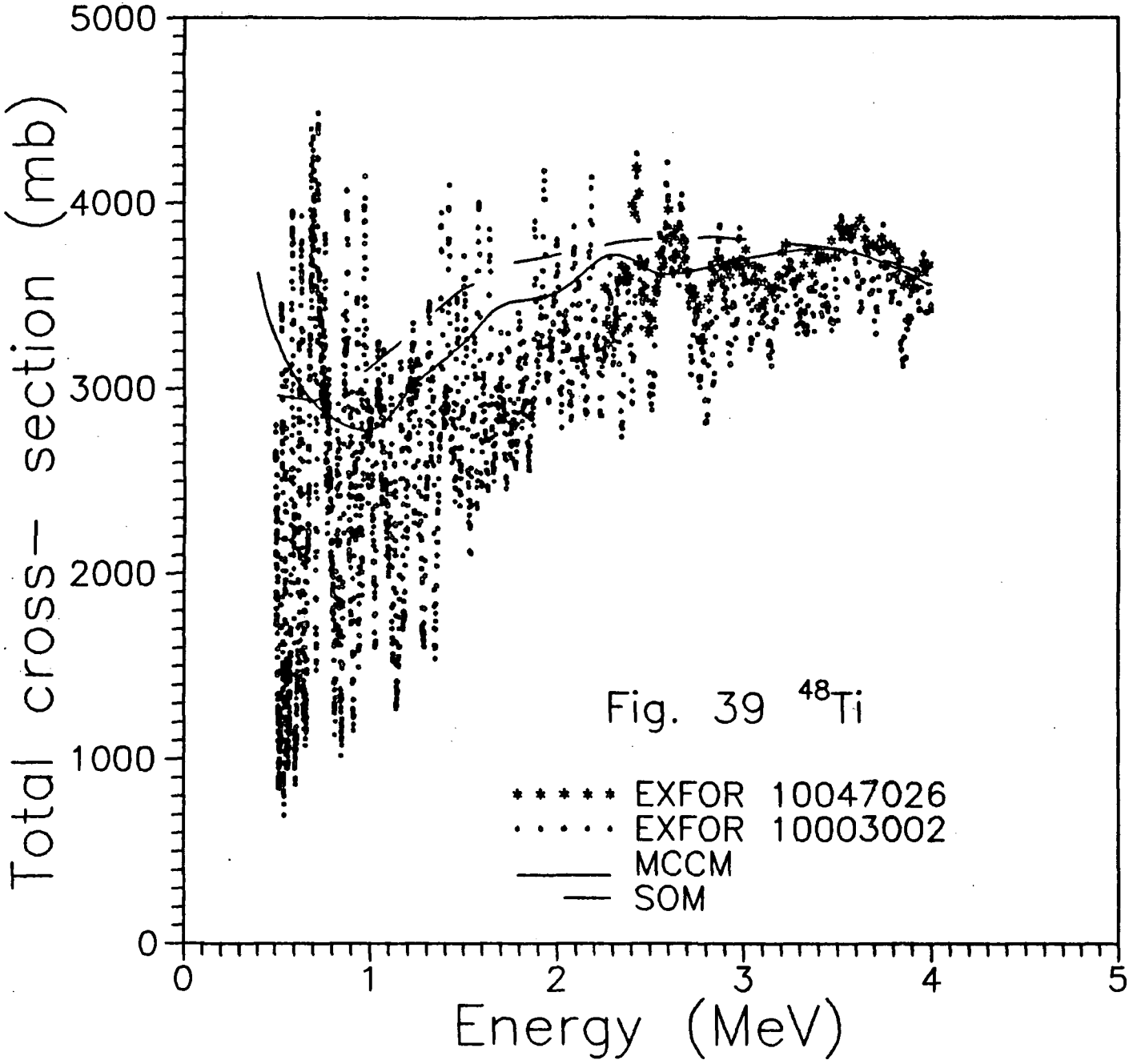
Total cross- section (mb)
5000
4000
3000
2000
1000
0
0
1
2
3
4
5
Energy (MeV)
Fig. 39 ^{48}Ti
EXFOR 10047026
EXFOR 10003002
MCCM
SOM

Reproduced by the IAEA in Austria
March 1992